Cancer Cell
Article

miR-296 Regulates Growth Factor Receptor Overexpression in Angiogenic Endothelial Cells

Thomas Würdinger,[1,2,5] Bakhos A. Tannous,[1,2] Okay Saydam,[1] Johan Skog,[1] Stephan Grau,[6] Jürgen Soutschek,[7] Ralph Weissleder,[2,3] Xandra O. Breakefield,[1,2,*] and Anna M. Krichevsky[4]
[1]Department of Neurology and Department of Radiology, Massachusetts General Hospital and Neuroscience Program
[2]Center for Molecular Imaging Research, Department of Radiology, Massachusetts General Hospital
[3]Center for Systems Biology, Massachusetts General Hospital
[4]Department of Neurology, Brigham and Women's Hospital
Harvard Medical School, Boston, MA 02115, USA
[5]Neuro-oncology Research Group, Department of Neurosurgery, VU Medical Center, Cancer Center Amsterdam, 1007 MB Amsterdam, The Netherlands
[6]Department of Neurosurgery, Klinikum Grosshadern, Ludwig-Maximilians-University Munich, 80539 Munich, Germany
[7]Regulus Therapeutics, Carlsbad, CA 92008, USA
*Correspondence: breakefield@hms.harvard.edu
DOI 10.1016/j.ccr.2008.10.005

SUMMARY

A key step in angiogenesis is the upregulation of growth factor receptors on endothelial cells. Here, we demonstrate that a small regulatory microRNA, miR-296, has a major role in this process. Glioma cells and angiogenic growth factors elevate the level of miR-296 in primary human brain microvascular endothelial cells in culture. The miR-296 level is also elevated in primary tumor endothelial cells isolated from human brain tumors compared to normal brain endothelial cells. Growth factor-induced miR-296 contributes significantly to angiogenesis by directly targeting the hepatocyte growth factor-regulated tyrosine kinase substrate (HGS) mRNA, leading to decreased levels of HGS and thereby reducing HGS-mediated degradation of the growth factor receptors VEGFR2 and PDGFRβ. Furthermore, inhibition of miR-296 with antagomirs reduces angiogenesis in tumor xenografts in vivo.

INTRODUCTION

Angiogenesis is the formation of new blood vessels during growth and development as well as in disease-related processes like tumor growth, wound healing, and restoring blood flow to tissues after injury (Folkman, 2007). De novo angiogenesis is a critical factor in cancer. For instance, malignant brain tumors are characterized by a marked increase in blood vessel formation, with tumor vessels having abnormal morphology that serves as a key feature in tumor grading (Brem et al., 1972; Folkerth, 2000). Increasing awareness of the importance of the vasculature in tumors has led to a focus on this as a therapeutic target (Kerbel and Folkman, 2002). The state of angiogenesis is a balance between pro- and antiangiogenic molecules, with a bias toward the proangiogenic mode (Jain, 2005). A common feature of angiogenic blood vessels is the high expression of proangiogenic growth factor receptors, such as platelet-derived growth factor receptor (PDGFR) and vascular endothelial growth factor receptor (VEGFR), which are targets of antiangiogenic therapies (Batchelor et al., 2007; Shih and Holland, 2006). Further understanding of the orchestration of this angiogenic switch should help in the development of strategies to harness the dynamics of blood vessel formation in human health and disease. Recently, the discovery of microRNAs (miRNAs) has increased our knowledge regarding the complex control of gene expression. miRNAs comprise a large group of endogenous noncoding RNAs that can block mRNA translation and/or negatively regulate its stability (Ambros, 2004). At this time, over 500 different miRNAs have

SIGNIFICANCE

The formation of new blood vessels by angiogenesis is essential for normal functions and is involved in many disease states, including cancer. Control of the angiogenic switch in endothelial cells involves changes in levels of pro- and antiangiogenic molecules acting in concert. Here, we show that glioma- or growth factor-mediated induction of miR-296 in endothelial cells results in increased levels of proangiogenic growth factor receptors. These results indicate that miR-296, belonging to the family of "angiomirs," is functionally linked to the angiogenic phenotype and therefore provide new insights into the role of miRNA regulation in neovascularization. Further, manipulation of miR-296 levels may prove therapeutic in the large number of diseases wherein angiogenesis is a critical component.

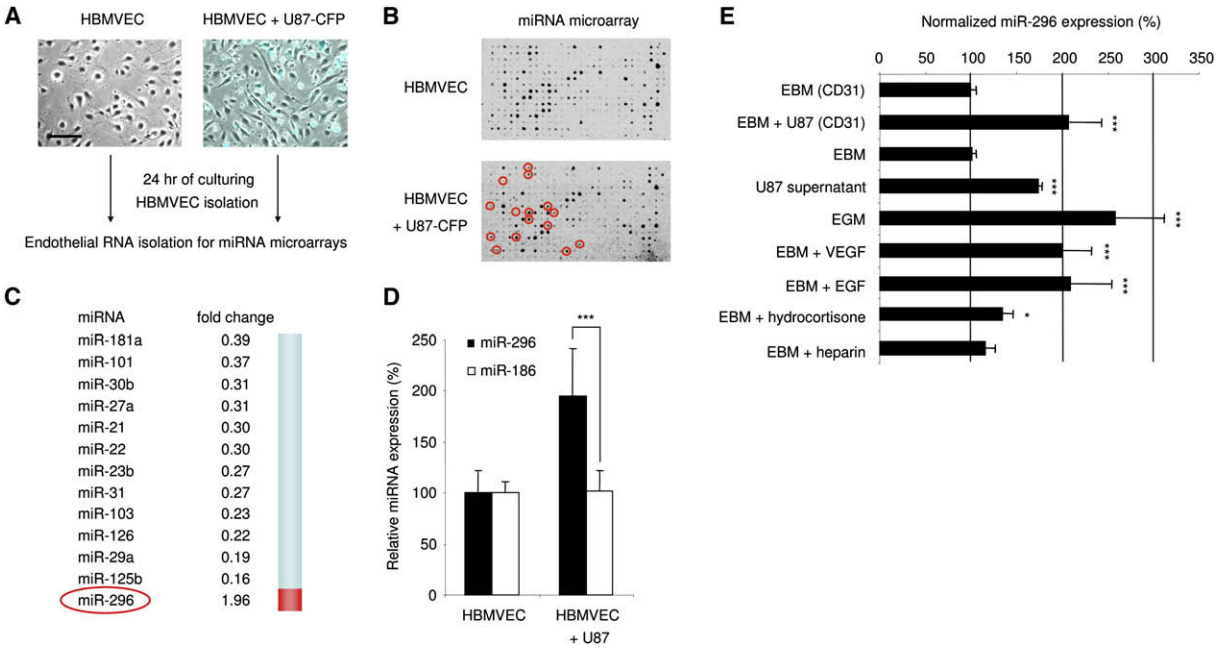

Figure 1. Glioma-Induced Dysregulation of miRNAs in Human Brain Endothelial Cells

(A) Primary human brain microvascular endothelial cells (HBMVECs) were cultured in the absence (left) or presence (right) of human U87-CFP glioma cells. Images were produced using a combination of light and fluorescence microscopy. Scale bar = 100 μm.

(B) Array hybridization analysis of miRNAs extracted from $CD31^+$ cells sorted from HBMVECs cultured without (upper array) or with (lower array) U87-CFP glioma cells for 24 hr. The density of the hybridization signals (black spots) reflects the relative expression level of particular miRNAs. Red circles indicate miRNAs that were significantly altered by coculture with glioma cells.

(C) A list of significantly decreased (fold change < 0.5) or increased (fold change > 1.9) miRNAs in HBMVECs exposed to U87-CFP glioma cells.

(D) Overexpression of miR-296 was confirmed by qRT-PCR analysis. RNA extracted from $CD31^+$ HBMVECs cultured in the absence or presence of U87 glioma cells was analyzed by qRT-PCR. The data were normalized to the level of GAPDH mRNA in each sample.

(E) HBMVECs were cultured in the presence or absence of U87 glioma cells, isolated using CD31 beads, and subjected to miR-296 qRT-PCR. Alternatively, HBMVECs were cultured in various culture media and subjected to miR-296 qRT-PCR. miR-296 levels were normalized to EBM (CD31).

Error bars indicate SD. *$p < 0.05$, ***$p < 0.001$ by t test.

been identified in human cells (Griffiths-Jones et al., 2006). Accumulating evidence indicates that regulation of miRNA levels is very important for proper growth and differentiation of many cell types and tissues (Bartel, 2004; Kloosterman and Plasterk, 2006; Krichevsky et al., 2003). It is also becoming clear that deregulated miRNA expression is a common feature of many human diseases, especially specific forms of cancer (Calin and Croce, 2006; Esquela-Kerscher and Slack, 2006; Ruvkun, 2006). Here, we aimed at identifying miRNAs that are critical to tumor angiogenesis.

RESULTS

Since glioma cells have a high capacity to induce angiogenesis (Brem et al., 1972; Folkerth, 2000), we used them as a means to stimulate this process in normal endothelial cells in a coculture system. Primary human microvascular endothelial cells isolated from normal human brain (HBMVECs; Cell Systems, ACBRI-376) were cultured in the presence or absence of human U87 glioma cells expressing cerulean fluorescent protein (CFP) in endothelial basal medium lacking additional angiogenic factors (EBM; Cambrex). Elongation of the endothelial cells was induced by the cancer cells as a first step in the activation of angiogenesis, as described previously (Khodarev et al., 2003) (Figure 1A). After 24 hr of either culturing the endothelial cells alone or coculturing them with human U87 glioma cells, the endothelial cells were isolated using CD31 magnetic beads (Dynal Biotech). The purity (>99%) of the endothelial cell preparation was confirmed by the absence of glioma cells expressing the CFP marker (data not shown). Total RNA was isolated from endothelial cells, and the small RNA fraction was hybridized to miRNA arrays containing probes for 407 mature miRNAs (as in Krichevsky et al., 2003) in order to identify differentially expressed miRNAs. Analysis of array hybridizations revealed 80 miRNAs expressed in HBMVECs at detectable levels (Figure 1B; see also Figure S1 available online) and confirmed the expression of a number of previously described miRNAs in endothelial cells (Kuehbacher et al., 2007; Poliseno et al., 2006; Suárez et al., 2007; Tuccoli et al., 2006). After exposure of HBMVECs to U87 glioma cells, the expression levels of a number of miRNAs changed significantly. This suggests that glioma cells can influence miRNA expression in endothelial blood vessel cells (Figures 1B and 1C). Most of the differentially expressed miRNAs were found to be downregulated. One miRNA, miR-296, was identified and further confirmed by quantitative RT-PCR (qRT-PCR) analysis to be upregulated. We used miR-186 as a control miRNA and GAPDH as a normalization control, both of which were uniformly expressed in endothelial cells in the presence or absence of tumor cells

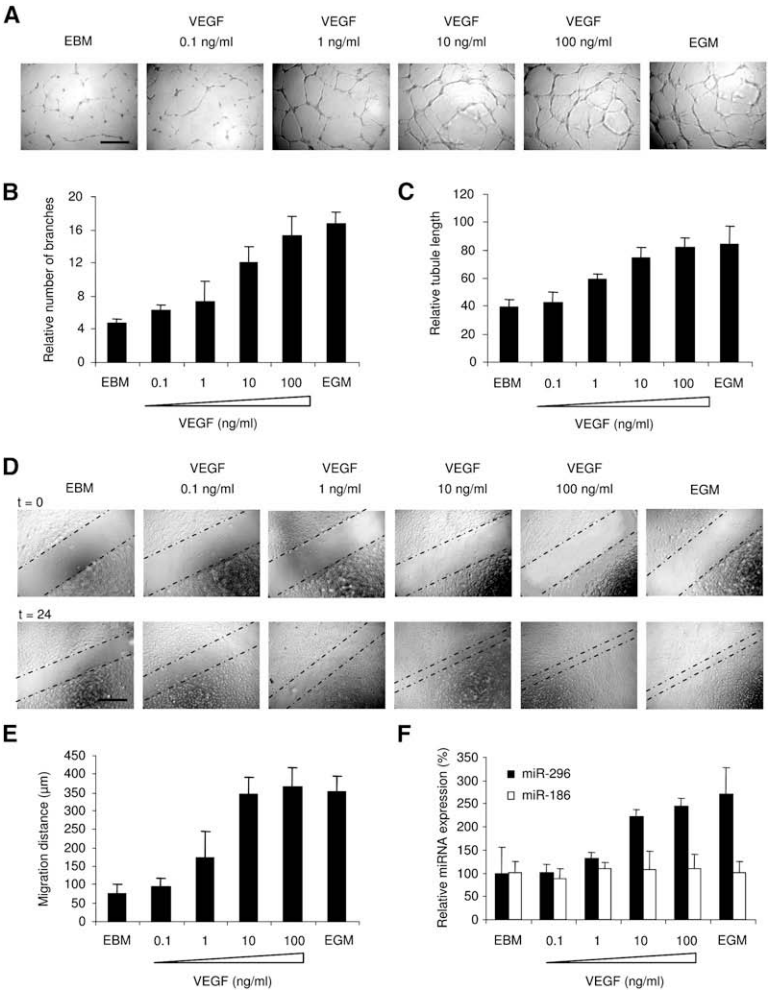

Figure 2. VEGF-Mediated Induction of Tubule Formation, Migration, and miR-296 Expression

(A–C) HBMVECs were cultured on Matrigel-coated plates in basal medium (EBM) only, basal medium supplemented with a cocktail of angiogenic factors (EGM), or different amounts of VEGF (A) and analyzed for tubule branching (B) and tubule length (C) after 24 hr. Scale bar in (A) = 300 μm.

(D) HBMVEC monolayer cultures were scratched and incubated as in (A). Directly after scratching (t = 0) and 24 hr later (t = 24), images were acquired. Dashed lines indicate the front of migration. Scale bar = 300 μm.

(E) Quantitation of migration distance using MetaVue software.

(F) HBMVECs were cultured as in (A) for 24 hr, after which RNA was isolated to determine the levels of miR-296 and miR-186 expression by qRT-PCR. The data were normalized to the level of GAPDH mRNA in each sample.

Error bars indicate SD.

(Figure 1D). In this study, we further investigated miR-296 since it was the only significantly upregulated miRNA in the glioma-induced endothelial cells.

In order to determine what factors are responsible for the induction of miR-296, HBMVECs were cultured using various conditions, after which RNA was isolated and miR-296 expression levels were determined. Of note, miR-296 was induced not only in HBMVECs upon exposure of these cells to U87 glioma cells but also by culture medium derived from U87 glioma cells and by EBM supplemented with angiogenic cocktail (EGM, containing hydrocortisone, EGF, FGF, VEGF, IGF, ascorbic acid, FBS, and heparin; SingleQuots from Cambrex). Similar ~2-fold induction of miR-296 in HBMVECs was achieved by EGM and glioma cell stimulation. Since U87-conditioned medium and EGM both contain many growth factors, HBMVECs were also stimulated with basal medium supplemented with VEGF or EGF, each of which resulted in significant miR-296 upregulation, in contrast to exposure to hydrocortisone and heparin, which did not change levels (Figure 1E).

Since VEGF enhanced miR-296 expression in endothelial cells, we addressed VEGF function in angiogenesis in endothelial cell culture. First, HBMVECs were cultured in the presence of different amounts of VEGF in EBM on a Matrigel substrate to promote tubule formation for 24 hr. A clear dose-response effect of VEGF on endothelial tubule formation and branching was observed (Figures 2A–2C). In order to determine whether endothelial cell migration was also affected by VEGF, scratch assays were performed. HBMVECs were first cultured in EGM, and a spatula was then used to scratch the monolayer, after which the cells were washed and cultured in EBM containing different amounts of VEGF, or in EGM, for 24 hr. VEGF significantly induced the migration of HBMVECs in a dose-responsive manner (Figures 2D and 2E). To determine a correlation between VEGF-induced phenotype and miR-296 expression, HBMVECs were cultured for 24 hr in EBM containing different amounts of VEGF, or in EGM, after which RNA was isolated and miR-296 expression levels were determined by qRT-PCR. Notably, 10 ng/ml of VEGF was sufficient to coordinately upregulate miR-296 levels and induce endothelial cell migration and tubule formation in HBMVEC cultures (Figures 2B, 2C, 2E, and 2F).

To address miR-296 function in angiogenesis, we examined the effects of its inhibition on glioma-induced angiogenesis in cell culture. In these experiments, HBMVECs were cultured on Matrigel in EBM alone, in EBM with human glioma cells, or in EGM. Tubules were visualized by a combination of light and fluorescence microscopy. Endothelial cells were discriminated from CFP-expressing U87 glioma cells by fluorescence microscopy (Figure 3A). miR-296 in endothelial cells was blocked by transfecting endothelial cells with a modified antisense miR-296 inhibitor (Ambion) prior to mixing the endothelial cells with U87 cells, with transfection efficiency being >99% as determined by transfection of siRNA-Cy3 (Alnylam) (Figure 3A). Levels of miR-296 decreased 4-fold in HBMVECs in the presence of this inhibitor as determined by qRT-PCR (Figure 3B). At 48 hr after transfection of the miR-296 inhibitor or a nonrelated oligonucleotide of similar chemistry and 24 hr of culturing on Matrigel with or without U87-CFP cells, endothelial cells were analyzed for effects on tubule length and tubule branching (Figure 3C). Downregulation of miR-296 resulted in a significant decrease in tubule branching (Figure 3D) and total tubule length (Figure 3E) in HBMVECs exposed to an angiogenic cocktail or U87 glioma cells as

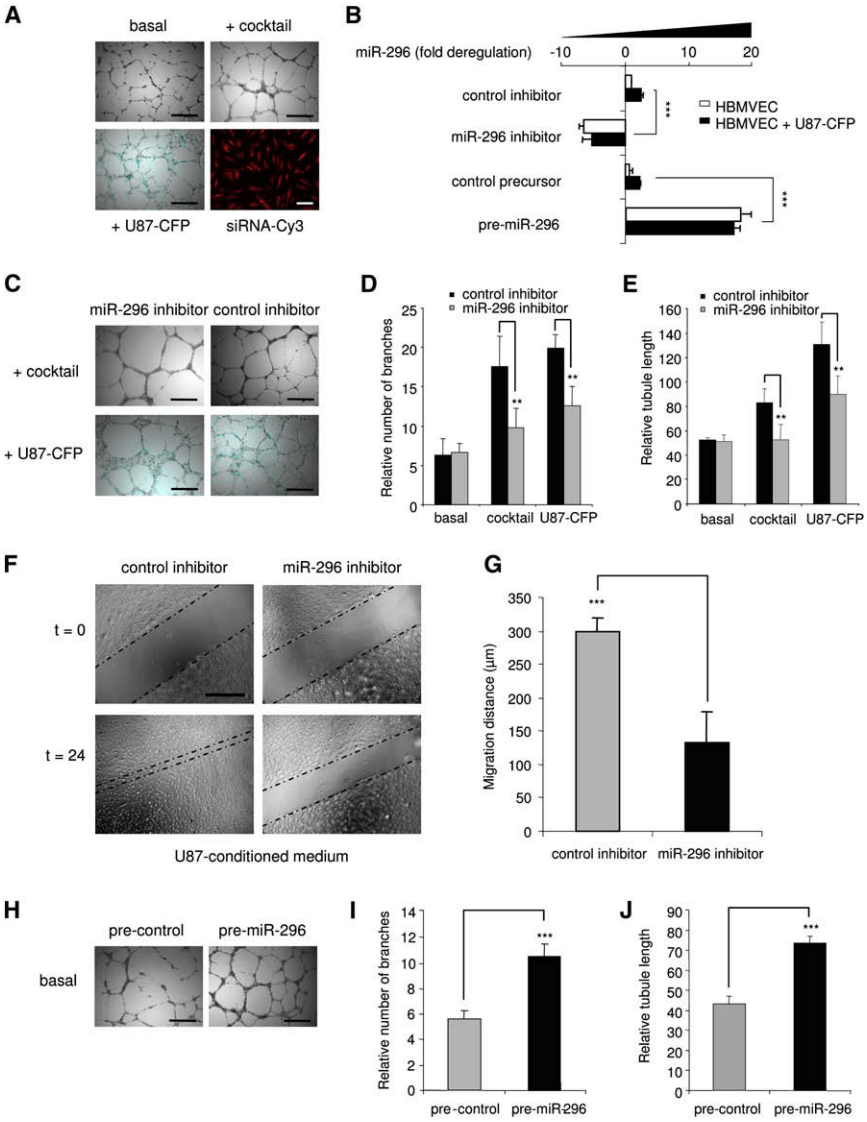

Figure 3. Angiogenesis Coculture Assay: miR-296-Mediated Inhibition and Induction of Angiogenesis

(A) HBMVECs were cultured on Matrigel-coated plates in basal medium (EBM) only, in basal medium supplemented with a cocktail of angiogenic factors (EGM), or with U87-CFP cells. Transfection efficiency of endothelial cells was determined (>99%) using siRNA-Cy3 molecules. Scale bars = 300 μm; monolayer culture scale bar in lower right panel = 50 μm.

(B) HBMVECs were transfected with anti-miR-296 inhibitor, pre-miR-296, or nonrelated control molecules and cultured in the presence or absence of U87-CFP cells. Inhibition and overexpression of miR-296 in $CD31^+$-isolated endothelial cells were quantified by qRT-PCR.

(C) HBMVECs were transfected with anti-miR-296 inhibitor or nonrelated control molecules and analyzed for tubule formation. Scale bars = 300 μm.

(D and E) Tubule formation was evaluated at 48 hr after transfection, including 24 hr of culturing on Matrigel, using the imaging program ImageJ. A significant decrease in tubule branching (D) and tubule length (E) was observed after transfection with miR-296 inhibitor.

(F and G) HBMVECs were transfected with anti-miR-296 inhibitor or nonrelated control molecules and analyzed for migration capacity (F). Inhibition of miR-296 resulted in a significant decrease in migration, as quantified in (G).

(H–J) Overexpression of miR-296 at 24 hr after transfection of pre-miR-296 molecules resulted in increased angiogenesis in vitro (H), as quantified by measuring tubule branching (I) and tubule length (J). Scale bars in (H) = 300 μm.

Error bars indicate SD. $^{**}p < 0.01$, $^{***}p < 0.001$ by t test.

compared to unexposed cells but had no significant effect on the viability of endothelial cells (Figure S2). U87 glioma cells induced tubule elongation to a greater extent than EGM, which may be due to other glioma cell-induced effects in addition to elevation of miR-296 (Figure 3E). Similar inhibitory effects on tubule formation were observed when miR-296 was blocked in human umbilical vein endothelial cells (HUVECs) exposed to an angiogenic cocktail (Figure S3), suggesting a general miR-296-mediated angiogenic mechanism operating in endothelial cells of different origins. In order to determine the effect of miR-296 inhibition on glioma-induced endothelial cell migration, scratch assays were performed. HBMVECs were transfected with the miR-296 inhibitor or control oligonucleotide. Twenty-four hours after transfection, a scratch was made in the monolayer of HBMVECs cultured in U87-conditioned medium. Twenty-four hours after that, the migration distance was analyzed by light microscopy and MetaVue software. Downregulation of miR-296 resulted in a significant decrease in U87-induced HBMVEC migration (Figures 3F and 3G).

To investigate whether miR-296 acts as a dominant determinant of angiogenesis, miR-296 precursor molecules or control precursor-like molecules (Ambion) were transfected into HBMVECs cultured in EBM medium. Transfection efficiency was >99% as analyzed by fluorescence microscopy using a precursor control molecule conjugated to a Cy3 fluorophor (Ambion) (data not shown). Overexpression of miR-296 in cells transfected with miR-296 precursors was confirmed by qRT-PCR (Figure 3B). Twenty-four hours after transfection, HBMVECs were plated on Matrigel in the absence of angiogenic stimuli. Pre-miR-296 stimulated tubule elongation and branching, in contrast to the control miRNA precursor (Figures 3H–3J). These effects were observed for up to at least 4 days after transfection of pre-miR-296 molecules into HBMVECs (Figure S4). Together, these data support a positive regulatory role for miR-296 in the induction of angiogenesis, i.e., miR-296 inhibition reduces the angiogenic phenotype, while miR-296 overexpression increases it.

To identify target genes regulated by miR-296 and involved in control of angiogenesis, we next evaluated targets computationally

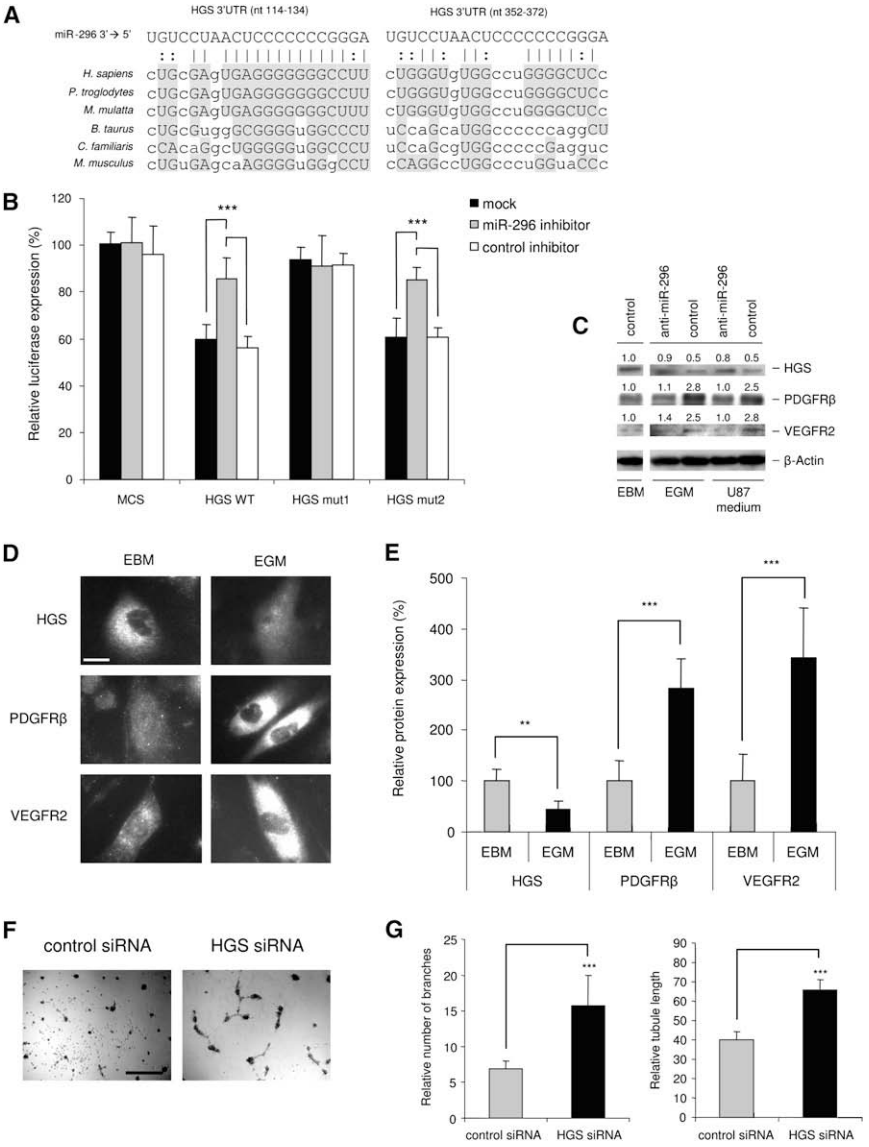

Figure 4. HGS Is a Direct Target of miR-296

(A) Alignment of potential miR-296 binding sites in the 3′UTR of the HGS mRNA of different species.

(B) pMir-Report vectors containing no 3′UTR (MCS) or containing the 3′UTR of the wild-type HGS mRNA (HGS WT) or mutated miR-296 binding sites (HGS mut1 and HGS mut2) and miR-296 or control inhibitors were cotransfected into HEK293T cells. The inhibition of miR-296 by the antisense inhibitors resulted in a significant increase in luciferase signals of HGS WT- and HGS mut2- but not HGS mut1-transfected cells.

(C) Western blot analysis of HGS, PDGFRβ, and VEGFR2 expression in HBMVECs cultured in basal medium (EBM) or HBMVECs stimulated by EGM or U87-conditioned medium. HGS expression decreased upon stimulation of HBMVECs, and PDGFRβ and VEGFR2 increased. Upon inhibition of miR-296 with anti-miR-296 molecules by transfection of HBMVECs stimulated by EGM or U87-conditioned medium, HGS expression increased, and PDGFRβ and VEGFR2 decreased. Relative blot intensities were quantified by using ImageQuant; densitometric values normalized to β-actin are indicated.

(D) HGS, PDGFRβ, and VEGFR2 expression levels under normal and angiogenic conditions. Representative images of HBMVEC immunostaining for HGS, PDGFRβ, and VEGFR2 under normal (EBM) and angiogenic (EGM) conditions are shown. Scale bar = 20 μm.

(E) Quantification of HGS, PDGFRβ, and VEGFR2 immunostaining levels as represented in (D). Fluorescence signals were quantified using MetaVue software by analyzing at least 20 random cells per sample.

(F and G) Silencing of HGS by siRNAs leads to increased HBMVEC tubule formation on Matrigel (F), as quantified in (G). Scale bar in (F) = 300 μm. Error bars indicate SD. **p < 0.01, ***p < 0.001 by t test.

predicted by publicly available algorithms (Griffiths-Jones et al., 2006; John et al., 2004; Krek et al., 2005; Lewis et al., 2005; Miranda et al., 2006). Interestingly, hepatocyte growth factor-regulated tyrosine kinase substrate (HGS) was one of the highest scored (according to miRBase, http://microrna.sanger.ac.uk; Griffiths-Jones et al., 2006) among the predicted miR-296 targets, with two potential conserved binding sites within its 3′UTR (Figure 4A). The HGS protein is involved in the regulation of levels of growth factor receptors, such as PDGFRβ (Takata et al., 2000) and VEGFR2 (Ewan et al., 2006). Upon ligand stimulation, phosphorylation, ubiquitination, and internalization of growth factor receptors, HGS mediates the sorting of these ligand/receptor complexes to lysosomes, where they are degraded (Bache et al., 2003; Ewan et al., 2006; Haglund et al., 2003; Raiborg et al., 2002; Stern et al., 2007; Takata et al., 2000). Elevated levels of growth factor receptors on the surface of endothelial cells, usually observed during tumor-induced angiogenesis, suggest a diminished role for HGS. In fact, silencing of HGS by siRNAs results in decreased degradation of growth factor receptors and hence their increased cellular levels (Bache et al., 2003; Stern et al., 2007). We hypothesized that miR-296 might downregulate synthesis of HGS by directly binding to sites within the 3′UTR of its message, thereby facilitating accumulation of angiogenic growth factor receptors. To test this hypothesis, we constructed luciferase reporter vectors encoding the complete wild-type 3′UTR of the HGS mRNA (HGS WT) as well as parallel control vectors containing mismatches in the predicted miR-296 binding sites (HGS mut1 and HGS mut2) or a luciferase vector containing no HGS UTR (MCS) and transfected these vectors into miR-296-expressing HEK293T cells (Miranda et al., 2006). Transfection of the HGS WT plasmid resulted in a decrease in luciferase expression (mock and control inhibitor) as compared to transfection of the MCS control (same conditions), supporting a negative effect of the endogenous miR-296 molecules on the HGS 3′UTR (Figure 4B). Blockage of endogenous miR-296 molecules using an antisense inhibitor (Ambion) resulted in a significant increase

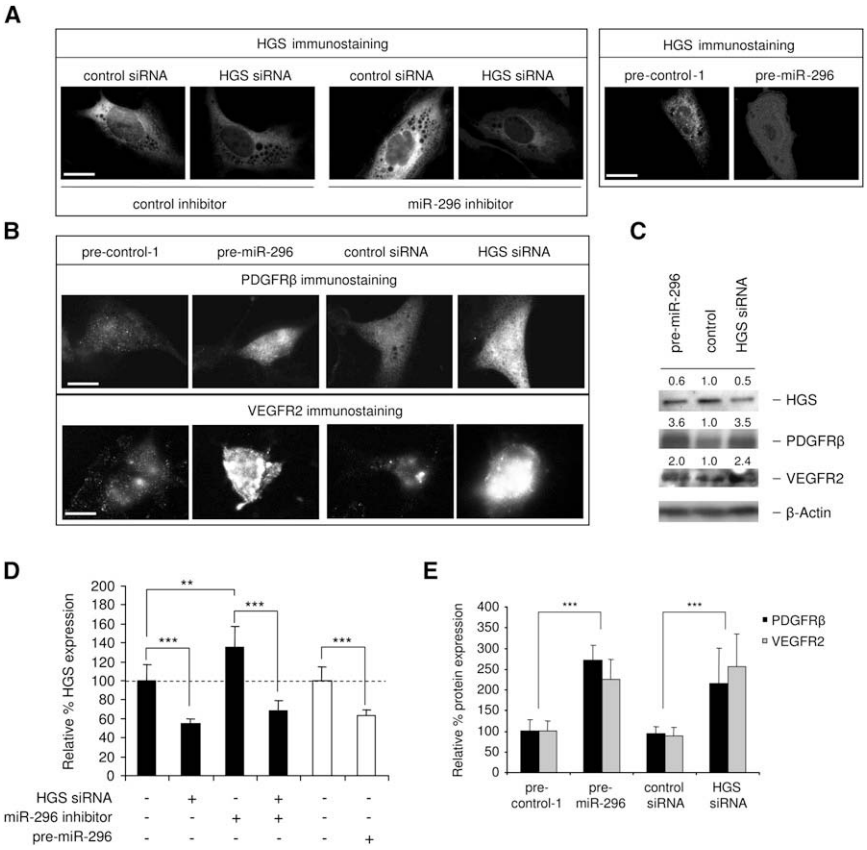

Figure 5. miR-296 Affects HGS-Modulated PDGFRβ and VEGFR2 Expression

(A) HGS immunostaining of HBMVECs after treatment with miR-296 inhibitors, anti-HGS siRNAs, and pre-miR-296 molecules. Scale bars = 20 μm.

(B) Immunostaining of PDGFRβ and VEGFR2 48 hr after transfection shows that transfection of pre-miR-296 molecules, as well as anti-HGS siRNAs, results in increased PDGFRβ and VEGFR2 expression in HBMVECs. Scale bars = 20 μm.

(C) Western blot analysis of HGS, PDGFRβ, and VEGFR2 expression in HBMVECs upon silencing of HGS by HGS siRNA or pre-miR-296. Relative blot intensities were quantitated by using ImageQuant; the densitometric values are indicated.

(D) Quantification of HGS immunostaining levels, as represented in (A).

(E) Increased cellular levels of immunoreactive PDGFRβ and VEGFR2 as seen in (B) were quantified using MetaVue software by analyzing at least 20 random cells per sample.

Error bars indicate SD. $^{**}p < 0.01$, $^{***}p < 0.001$ by t test.

in HGS WT luciferase expression (Figure 4B). Mutations in the predicted miR-296 binding site 1 (nt 114–134; HGS mut1, Figures 4A and 4B) caused a loss of luciferase sensitivity to miR-296 inhibition as compared to HGS WT, while HGS mut2 with a mutation in miR-296 binding site 2 (nt 352–372) did not. These experiments validated the regulatory potential of miR-296 via binding site 1, which has a better predicted base-pairing and is more evolutionarily conserved relative to binding site 2 within the HGS 3′UTR.

In order to confirm miR-296-mediated modulation of endogenous HGS in endothelial cells, HBMVECs were transfected with miR-296 inhibitor or control molecules and cultured in EGM or U87-conditioned medium. After 48 hr, the cell lysates were analyzed for HGS expression levels by western blotting. Inhibition of miR-296 resulted in increased levels of HGS (Figure 4C). To determine whether HGS protein levels were reduced in angiogenic endothelial cells, HBMVECs were cultured in EBM, EGM, or U87-conditioned medium. After 24 hr, HGS, PDGFRβ, and VEGFR2 protein expression levels were determined by western blotting and normalized to β-actin levels. HBMVECs cultured in the angiogenesis-inducing (and miR-296-inducing) EGM or U87-conditioned medium exhibited decreased HGS expression levels and increased PDGFRβ and VEGFR2 expression levels (Figure 4C). In parallel, HGS as well as PDGFRβ and VEGFR2 protein expression levels were determined under normal (EBM) and angiogenic (EGM) conditions by immunostaining. Immunostaining (Figure 4D) and quantitation of the fluorescence intensities (Figure 4E) showed that the HGS protein level was decreased at least 2-fold by angiogenic factors, whereas the PDGFRβ and VEGFR2 protein levels were increased about 3-fold. These results show that HGS is downregulated under angiogenic conditions (in which miR-296 is upregulated), with this reduction being prevented by blocking miR-296, and with HGS expression levels being inversely correlated with PDGFRβ and VEGFR2 levels. To further confirm the functional effect of HGS on angiogenesis, HGS siRNAs (QIAGEN) or control siRNAs were transfected in HBMVECs. After 24 hr, the transfected HBMVECs were cultured in EBM on Matrigel. Silencing of HGS resulted in increased tubule formation and branching (Figures 4F and 4G), supporting critical involvement of HGS in the angiogenic process.

Importantly, antisense inhibition of miR-296 resulted in a moderate but significant increase in levels of endogenous HGS in HBMVECs, and this effect was abolished by cotransfection with a siRNA directed against HGS as shown by immunofluorescence visualization (Figure 5A) and quantification of average fluorescence intensities (Figure 5D). In addition, overexpression of miR-296 resulted in moderate but also significant downregulation of HGS expression (Figures 5A and 5D). The knockdown of HGS by siRNA or pre-miR-296 was confirmed by western blots (Figure 5C). Notably, when HGS levels were decreased by either siRNA or pre-miR-296 transfection, a significant increase in PDGFRβ and VEGFR2 protein levels was observed by immunofluorescence staining (Figures 5B and 5E) and confirmed by western blots (Figure 5C), consistent with downregulation of HGS by miR-296, which in turn reduces degradation of the growth factor receptors. Both down- and upregulation of miR-296 appear to be physiologically relevant, since they affected the levels of downstream proteins (HGS, VEGFR2, and PDGFRβ) within the physiologically relevant range observed in angiogenic versus nonangiogenic conditions.

In order to confirm that HGS-regulated growth factor receptors are functional in glioma-induced angiogenesis, VEGFR2 receptor antibody blocking experiments were performed.

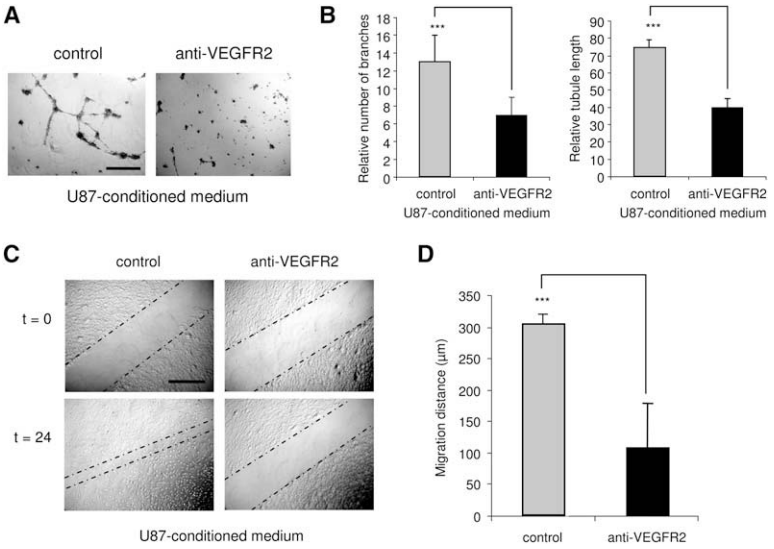

Figure 6. Blocking of VEGFR2 Reduces Angiogenesis In Vitro

(A) HBMVECs were stimulated using U87-conditioned medium and cultured on Matrigel-coated plates in the presence or absence of VEGFR2-blocking antibody. Scale bar = 300 μm.

(B) After 24 hr, VEGFR2 blocking significantly reduced tubule branching and tubule length.

(C and D) HBMVECs were cultured in a monolayer, scratched, and incubated in the presence or absence of VEGFR2-blocking antibody for 24 hr (C). VEGFR2 blocking resulted in a significant decrease in HBMVEC migration, as quantified in (D). Scale bar in (C) = 300 μm.

Error bars indicate SD. ***$p < 0.001$ by t test.

HBMVECs were cultured in U87-conditioned medium. After 24 hr, the HBMVECs were transferred onto Matrigel and cultured in U87-conditioned medium in the presence or absence of VEGFR2-blocking antibody (1 μg/ml). After 24 hr, a significant decrease in tubule length and branching was observed in the presence, as compared to the absence, of these antibodies (Figures 6A and 6B). In addition, scratch motility assays were performed using HBMVECs cultured in the presence or absence of VEGFR2-blocking antibody. After 24 hr, a significant reduction in the migration distance was observed upon incubation of the HBMVECs in the presence of VEGFR2 antibody (Figures 6C and 6D). These results indicate that functional VEGFR2 expression contributes to the angiogenic phenotype of HBMVECs stimulated by U87-conditioned medium.

To analyze whether miR-296 affects glioma angiogenesis in vivo, a synthetic cholesterol-conjugated antagomir-296 antisense oligonucleotide was designed. U87 glioma cells were injected in the back flanks of nude mice. After 7 days of tumor growth, antagomir-296 or mismatch control antagomir was injected intravenously into these mice (100 μl of a 20 mg/ml stock diluted in PBS). At 4 days after injection of the antagomirs, AngioSense 750 (VisEn Medical) was injected intravenously in order to quantify neovascularization by fluorescence-mediated tomography (Montet et al., 2007). The mice injected with antagomir-296 showed a significant decrease in mean fluorescence intensity in their tumors as compared to the mice injected with the mismatch control (Figures 7A and 7B). T1-weighted magnetic resonance (MR) images were also acquired to show the tumor volume (Figure 7C). These

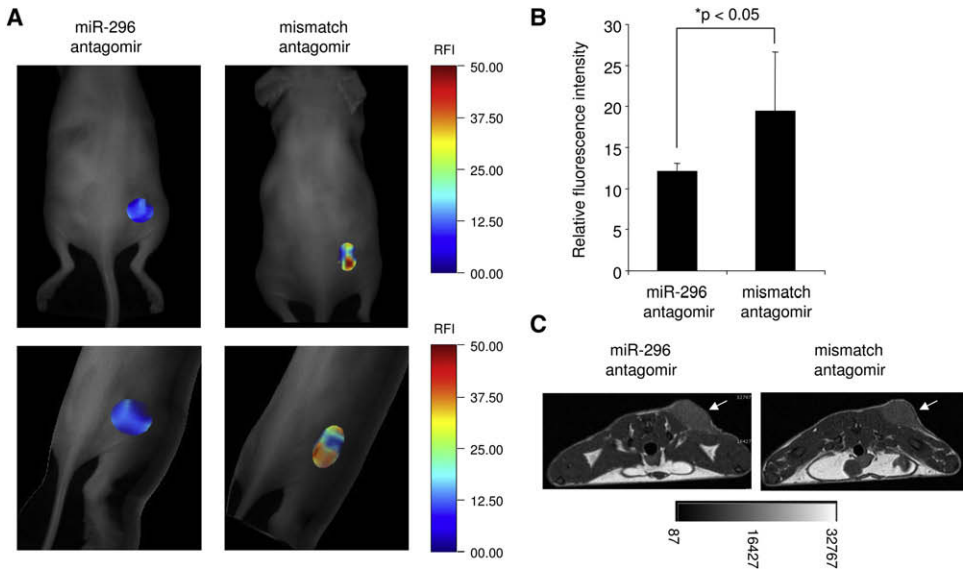

Figure 7. In Vivo Analysis of miR-296 Inhibition of Tumor Neovascularization

(A) Mice with subcutaneous U87 tumors (n = 6) were injected intravenously with miR-296 antagomirs or mismatch control antagomirs. Four days later, the same mice were injected with AngioSense 750, and tumor vasculature was analyzed by fluorescence-mediated tomography (FMT). Planar (top) and 3D FMT (bottom) images are displayed in which the fluorescence signals are superimposed with the grayscale planar excitation light image of the mouse. RFI, relative fluorescence intensity.

(B) Quantitation of the mean fluorescence intensity measurements from tumors in (A) using OsiriX. Error bars indicate SD. *$p < 0.05$ by t test.

(C) Transverse T1-weighted magnetic resonance (MR) images (4.7T) acquired to show the tumor volume in (A). White arrows indicate tumor mass.

A

Patient #1	NNB	trauma	frontal
Patient #2	NNB	seizures	temporal
Patient #3	NNB	seizures	temporal
Patient #4	WHO°II	diffuse astrocytoma	temporal
Patient #5	WHO°II	gemistocytic astrocytoma	frontal
Patient #6	WHO°II	diffuse astrocytoma	frontal
Patient #7	WHO°IV	GBM	temporal
Patient #8	WHO°IV	GBM	frontal
Patient #9	WHO°IV	GBM	parietal

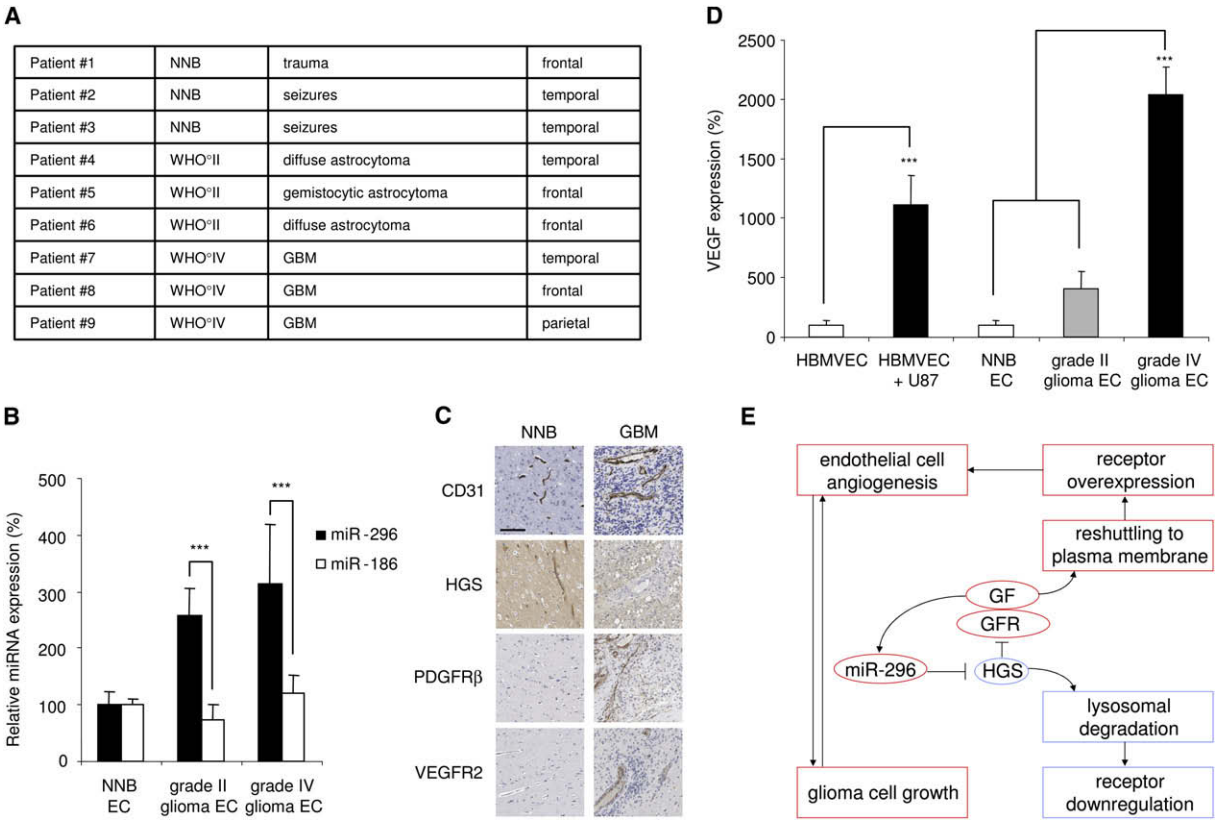

Figure 8. Analysis of Expression of miR-296 and Its Targets in Tumor Endothelial Cells Isolated from Human Gliomas

(A) RNA was isolated from primary endothelial cell cultures (passage 0) prepared from normal human brain (NNB; n = 3), grade II astrocytomas (n = 3), and grade IV glioblastoma multiforme (n = 3).

(B) RNA extracted from individual tumor endothelial samples was analyzed by qRT-PCR for expression levels of miR-296 and miR-186. All values were normalized to GAPDH mRNA levels in the same samples.

(C) Immunohistochemical staining of brain blood vessels indicates increased and morphologically abnormal tumor blood vessels as well as differential HGS, PDGFRβ, and VEGFR2 expression in nonneoplastic brain (NNB) and malignant glioma (GBM). Scale bar = 100 μm.

(D) RNA extracted from individual tumor endothelial samples was analyzed by qRT-PCR for expression levels of VEGF. All values were normalized to GAPDH mRNA levels in the same samples. Error bars in (B) and (D) indicate SD. ***$p < 0.001$ by t test.

(E) Schematic overview of the proposed angiogenic mechanism of miR-296. miR-296 is upregulated in glioma endothelial cells and directly inhibits expression of HGS, thereby allowing the accumulation of growth factor receptors by attenuating their degradation. GF, growth factor; GFR, growth factor receptor.

results demonstrate that inhibition of miR-296 affects glioma angiogenesis in vivo.

In order to establish the clinical relevance of miR-296 regulation in glioma angiogenesis, we performed experiments on human endothelial cells isolated from tumor tissue obtained from neurosurgical resections. Endothelial cells were isolated from blood vessels dissected from six glioma patients (three grade IV gliomas [highly malignant] and three grade II gliomas [less malignant]), all of which were highly angiogenic as confirmed by CD31 immunohistochemical analysis in pathological specimens (data not shown), as well as from three normal nonneoplastic human brain samples (Figure 8A). miR-296 expression levels, determined by qRT-PCR, were elevated in tumor blood vessels relative to quiescent normal brain vessels (Figure 8B), while control miR-186 showed no difference in expression levels. We further examined expression of HGS, PDGFRβ, and VEGFR2 proteins in endothelial cells from human nonneoplastic brain and malignant gliomas. Immunohistochemical staining revealed that HGS expression was low and PDGFRβ and VEGFR2 were upregulated in angiogenic glioma blood vessels relative to normal control vessels (Figure 8C). Finally, using qRT-PCR, we determined mRNA levels of VEGF in endothelial cells isolated from nonneoplastic human brain and glioma tissues, as well as in HBMVECs cultured in the presence or absence of U87 glioma cells. A clear increase in VEGF mRNA was observed in tumor endothelial cells and in U87-exposed HBMVEC cultures as compared to these controls (Figure 8D), paralleling miR-296 expression levels. These data suggest that growth factor-induced miR-296 expression observed in cultured brain endothelial cells parallels changes in miR-296 levels in angiogenic endothelial cells in brain tumors in vivo. Furthermore, miR-296 downregulation of HGS signaling increases functional PDGFRβ and VEGFR2 in tumors, which is complemented by increased expression of VEGF.

DISCUSSION

Altogether, our results support a role for miR-296 in promoting angiogenesis in tumors. We show that VEGF alone is capable

of increasing miR-296 to levels equivalent to those reached with growth factor-supplemented endothelial medium or glioma cells. This result points out an interesting feedback loop whereby VEGF induces miR-296 expression, which targets HGS, which in turn results in increased VEGFR2 and PDGFRβ protein levels and hence increased response to VEGF. In addition, EGF was also capable of inducing miR-296, suggesting a complex growth factor-growth factor receptor crosstalk mechanism that combinatorially increases miR-296 levels.

miR-296 was identified in a miRNA screen in normal human brain endothelial cells as being upregulated in response to exposure to human brain glioma cells in culture. Down- and upregulation of miR-296 resulted in the inhibition and induction, respectively, of morphologic characteristics associated with angiogenesis of human endothelial cells. Sequence-specific inhibition of miR-296 by intravenous injection of cholesterol-conjugated antagomirs resulted in decreased neovascularization of tumors in mice. Upregulation of miR-296 expression was also demonstrated in tumor blood vessels isolated from human glioblastoma tumors. Altogether, these results support a role for increased miR-296 levels in promoting angiogenesis in tumors, as illustrated in the model in Figure 8E. It is likely that other endothelial miRNAs have related pro- or antiangiogenic functions. A proangiogenic role for miR-296 was demonstrated for HBMVECs as well as HUVECs; however, since miRNAs have multiple targets, miR-296 may also play important roles in other physiological processes unrelated to angiogenesis. We propose that in the endothelial context, miR-296 belongs to the family of "angiomirs." Kuehbacher et al. (2007) have shown that inhibition of let-7f and miR-27b also affects angiogenesis. Recently, miR-126 was found to play an important role in developmental angiogenesis and vascular integrity (Fish et al., 2008; Wang et al., 2008). We have detected several members of the let-7 family, as well as miR-27 and miR-126, in HBMVECs (Figure S1). Under conditions used in our study, these miRNAs appeared to be downregulated in HBMVECs exposed to glioma cells. Understanding functions of these miRNAs and their contribution to tumor angiogenesis will require further investigation. Thus, although several miRNAs have been implicated in endothelial processes in vitro (Chen et al., 2008; Kuehbacher et al., 2007; Lee et al., 2007; Poliseno et al., 2006; Suárez et al., 2007; Dews et al., 2006) and in vivo (Fish et al., 2008; Wang et al., 2008), miR-296 plays a functional role in human tumor-induced angiogenesis in vitro and in vivo.

We have confirmed that the mRNA for HGS is a target for miR-296. Our data suggest that miR-296 upregulation has a dominant downtuning effect on HGS expression in angiogenic endothelial cells, although additional regulatory factors (including miRNAs) can not be excluded. Since HGS mediates the degradative sorting of PDGFR (Takata et al., 2000) as well as VEGFR (Ewan et al., 2006) and EGFR (Bache et al., 2003; Stern et al., 2007), it seems likely that increased levels of these growth factor receptors in angiogenic blood vessels are due at least in part to the miR-296 downregulation of HGS expression.

In recent years, a number of oncomirs (tumor-promoting miRNAs) and tumor-suppressing miRNAs have been identified for various types of cancer cells (reviewed in Esquela-Kerscher and Slack, 2006; Wurdinger and Costa, 2007). However, the delivery of inhibitors or precursor/mimics of such miRNAs to cancer cells in order to block tumor growth remains challenging. Tumor blood vessels offer an attractive additional target for the delivery of miRNA inhibitors or precursor/mimics in order to reduce tumor growth. Recent delivery configurations using siRNA-based and miRNA-inhibiting antagomirs have proved effective for miRNA manipulation in vivo, and blood vessels are a feasible target for such molecules in vivo (de Fougerolles et al., 2007; Krutzfeldt et al., 2005). Several siRNAs can target the vasculature, resulting in alterations in blood vessel structure and function (Reich et al., 2003; Shen et al., 2006). These siRNAs are aimed at silencing single specific mRNA targets but may have off-target side effects (Jackson et al., 2003). miRNAs such as miR-296, however, can regulate a broad range of "natural" mRNA targets (Miranda et al., 2006) and might therefore prove more efficient for fine tuning cellular switch programs. Our results indicate that miR-296 is a critical component of the angiogenic process, possibly in a one-hit/multiple-target fashion (Wurdinger and Costa, 2007), and provide insights into the role of miRNA regulation of neovascularization. Furthermore, manipulation of angiomir levels may prove therapeutic in the vast number of diseases in which angiogenesis is a critical component.

EXPERIMENTAL PROCEDURES

Cells

Human brain microvascular endothelial cells (HBMVECs; Cell Systems, ACBRI-376) and human umbilical vein endothelial cells (HUVECs; Cambrex) were cultured in EGM medium (Cambrex) for no more than ten passages. U87 cells (ATCC; U87 MG) and 293T cells were cultured in DMEM containing 10% FBS and antibiotics. U87-CFP cells were produced by stably transducing U87 cells with a CMV-controlled cerulean expression cassette using a lentiviral vector (Rizzo et al., 2004).

Endothelial Cell Isolation

Endothelial cells were isolated from HBMVECs cultured for 24 hr alone or in the presence of glioma cells using CD31 Endothelial Cell Dynabeads (Dynal Biotech). Cells were trypsinized, and trypsin was then inactivated using trypsin neutralization solution (Cambrex). Single-cell suspensions containing 1×10^6 cells were washed once in PBS and resuspended in 1 ml PBS, to which 25 μl of CD31 Dynabeads was added. The tubes were subjected to slow rotation for 20 min at 4°C. Subsequently, the tubes were placed in a magnet for 2 min and washed three times with 1 ml PBS containing 0.1% BSA. Isolated endothelial cells were plated in EGM medium and analyzed for presence of U87-CFP contamination using a combination of light and fluorescence microscopy. Only an occasional sporadic U87-CFP cell was observed, indicating >99.9% purity of the endothelial cell population. Endothelial cells were also isolated from blood vessels dissected from three grade IV gliomas and three grade II gliomas, as well as from normal nonneoplastic human brain. All endothelial cell isolations from normal human brain and glioma tissue were performed using CD31 and VE-cadherin magnetic-activated cell sorting (MACS), and >99% purity of cell isolations was confirmed by UEA-1 binding and 1,1′-dioctadecyl-3,3,3′,3′-tetramethylindocarbocyanine perchlorate-acetylated low-density lipoprotein (Ac-Dil LDL) uptake as described previously (Miebach et al., 2006).

RNA Isolation

Total RNA was isolated from endothelial cells passaged fewer than seven times in culture and primary endothelial cells (passage 0) isolated from normal brain and glioma tissue. RNA isolation was carried out by adding 600 μl of lysis buffer from a mirVana miRNA isolation kit (Ambion) to the CD31 bead-bound cells. The quality and quantity of the RNA were analyzed by photospectrometry and analytical 15% TBE-UREA gels (Bio-Rad) after ethidium bromide staining.

miRNA Inhibition and Overexpression

For the inhibition of miR-296, 50 nM miR-296 inhibitor oligonucleotide (Ambion) or control oligonucleotides were transfected into HBMVECs or HUVECs

using Lipofectamine 2000 (Invitrogen). For overexpression of miR-296, 50 nM pre-miR-296, pre-control-Cy3, or pre-control-1 (Ambion) was transfected into HBMVECs. After 5 hr, the cells were trypsinized, replated, and cultured in EBM or EGM until further analysis.

In Vitro Glioma Angiogenesis Assay

HBMVECs or HUVECs (both passaged fewer than seven times) were cultured on Matrigel (Becton Dickinson) in EBM (Cambrex) in the presence or absence of U87-CFP cells or EGM (Cambrex). After 24 hr, the cultures were analyzed by a combination of light and fluorescence microscopy. The experiments were performed in triplicate, repeated at least twice, and judged in a double-blind fashion by at least two observers. Three or more random pictures were taken of each culture using a digital camera system and the software program MetaVue (Molecular Devices), and images were subsequently analyzed for total tubule length and number of tubule branches using the software program ImageJ.

In Vitro Migration Scratch Assay

Confluent HBMVECs (passaged fewer than seven times) were transfected with miR-296 mimics, inhibitors, or control oligonucleotides using Lipofectamine 2000 (Invitrogen). At 5 hr after transfection, a cell scratch spatula was used to make a scratch in the cell monolayer, after which the cell monolayers were rinsed and further incubated. Pictures of the scratches were taken using a digital camera system coupled to a microscope. The cells were incubated for 24 hr, after which pictures were taken again. MetaVue was used to determine the migration distance (in μm) as the reduction of the width of the open area.

Luciferase miRNA Target Reporter Assay

Total cDNA from HBMVECs was used to isolate the 3′UTR of *Hgs* by PCR using the forward primer 5′HGS TTGACTAGTCCCAGGCCATGCTCACGTCCG GAGTAACACTAC and the reverse primer 3′HGS TTGAAGCTTGAAATACAT TTTATTATCGCTGTACCATTCTGGGG. After digestion of the PCR product by SpeI and HindIII, the *Hgs* 3′UTR was cloned into the SpeI and HindIII sites of the multiple cloning site (MCS) of pMir-Report (Ambion), resulting in pMir-Report-3′HGS. Mutations were introduced in the potential miR-296 114–134 and 352–372 binding sites (Figure 3A). The flanking primers that were used for the isolation of the *Hgs* 3′UTR from the endothelial cDNA were combined with primers containing mutated target sequences. For the 5′ (pMir-Report-3′HGS-mut114–134, denoted HGS mut1) miR-296 binding site, primers used were mutP1AF: CAACCTGACTAAAACCCGGAACACCCCAAGCCCACC TCCCTTGTCCTCAG and mutP2AR: TTCCGGGTTTTAGTCAGGTTGAGAAG GGACACTACCGGCAGTAGAGGACA. For the downstream (pMir-Report-3′HGS-mut352–372, denoted HGS mut2) miR-296 binding site, primers used were mutP1BF: CACAATGACACCTCCCCGAGCCTCTGCAGGGGCCT CTCTCGGCAGCCACA and mutP2BR: GCTCGGGGAGGTGTCATTGTGAC ACCACAGCCAGCTCACAGTGCGGCCAG. 293T cells were transfected with the pMir-Report vectors containing the wild-type *Hgs* and variant 3′UTRs, and at 5 hr after transfection, the cells were transfected again with 50 nM miR-296 inhibitors (Ambion) or control oligonucleotides (Ambion). After 24 hr, the cells were lysed and luciferase activity was measured using a luminometer. A plasmid containing an expression cassette for *Renilla* luciferase, pRenilla (Promega), was cotransfected and used to normalize the firefly luciferase values expressed from the pMir-Report constructs.

Immunofluorescence Staining and Western Blotting

Cell cultures were fixed using PBS containing 4% paraformaldehyde for 15 min at room temperature (RT) and (for HGS) permeabilized using PBS containing 1% Triton X-100 for 5 min at RT. Nonspecific antibody binding was blocked by incubating the cells in PBS containing 5% FCS for 30 min at RT. Mouse monoclonal anti-HGS (1:100, Alexis Biochemicals), anti-PDGFRβ (1:50, BD Biosciences), and anti-VEGFR2 (1:400, Abcam) antibodies were used to detect HGS, PDGFRβ, and VEGFR2, respectively. Donkey anti-mouse-Cy3 (1:600, Jackson Immunolabs) was used as a secondary antibody. Immunofluorescence was analyzed using fluorescence microscopy. Immunohistochemical analysis of CD31 was performed as described previously (Miebach et al., 2006). For western blotting, cells were grown for 24 hr and lysed by standard procedure in RIPA buffer containing protease inhibitor cocktail (Roche Diagnostics). Protein concentrations of total cell lysates were measured using a Micro BCA Protein Assay Kit (Pierce Biotechnology), and 40 μg of tissue culture lysate per lane was resolved on SDS-PAGE gels (Invitrogen) followed by immunoblot detection and visualization with ECL western blotting detection reagents (Pierce Biotechnology). The bands of the western blots were quantitated using ImageQuant software (Molecular Dynamics). The intensities were normalized to anti-β-actin levels and depicted as relative intensities. Immunoblotting was performed with the primary antibodies mouse anti-HGS (1:1000, Alexis Biochemicals), mouse anti-PDGFRβ (1:1000, Abcam), mouse anti-VEGFR2 (1:1000, Abcam), and mouse anti-β-actin (1:5000, Abcam). In addition, http://www.proteinatlas.org/ was used as a source of immunohistochemical analysis for CD31, HGS, PDGFRβ, and VEGFR2 protein expression.

Quantitation of HGS, PDGFRβ, and VEGFR2 Expression in Cells Treated with siRNAs

The expression levels of HGS, PDGFRβ, and VEGFR2 were measured as immunofluorescence intensity per cell. The experiments were performed in triplicate, repeated at least twice, and judged in a double-blind fashion by at least two observers. Twenty or more random pictures (one cell per field) were taken using a Nikon fluorescence microscope system coupled to a digital camera and analyzed using MetaVue. The values of the HGS, PDGFRβ, and VEGFR2 average intensities were averaged. Error bars denote SD, and t test was used to determine significant differences.

In Vivo Imaging of Angiogenesis

All experiments on mice were approved by the Subcommittee on Research Animal Care at Massachusetts General Hospital and were performed in accordance to their guidelines and regulations. One million U87 cells were mixed with 50 μl Matrigel (Becton Dickinson) and directly injected subcutaneously into the back flanks of nude mice. After 7 days, each mouse was injected intraocularly with 2 mg of miR-296 antagomirs or mismatch control antagomirs (100 μl of a 20 mg/ml stock diluted in PBS; Regulus Therapeutics). Four days after injection of antagomirs, 150 μl (2 nmol fluorochrome) of AngioSense 750 (VisEn Medical) was injected intravenously. One hour later, coronal fluorescence-mediated tomography (FMT) images were acquired using a continuous wave-type scanner capable of acquiring transillumination, reflectance, and absorption data (VisEn Medical). Prototypes of the device and reconstruction algorithms, as well as the imaging protocol, have been described previously (Montet et al., 2005, 2007; Ntziachristos et al., 2002; Grimm et al., 2005). Mice were also imaged by magnetic resonance (MR) using a 4.7T small-animal MR scanner (Bruker BioSpin). The imaging protocol consisted of an axial T1-weighted sequence with the following parameters: fast spin echo 635/15 ms repetition time/echo time, four averages, matrix slice 256 × 128, field of view 4.0 × 2.5 cm, slice thickness 1 mm. Sixteen slices with a slice thickness of 1 mm, field of view of 42 × 24 mm, and matrix of 128 × 64 were acquired.

ACCESSION NUMBERS

The miRNA array data described herein have been deposited in the NCBI Gene Expression Omnibus (http://www.ncbi.nlm.nih.gov/geo/) with the accession number GSE13091.

SUPPLEMENTAL DATA

The Supplemental Data include Supplemental Experimental Procedures, Supplemental References, and four figures and can be found with this article online at http://www.cancercell.org/supplemental/S1535-6108(08)00329-2.

ACKNOWLEDGMENTS

We would like to acknowledge the Steve Kaplan Fellowship from the American Brain Tumor Association (T.W.); NIH grants NCI P50 CA86355-04 (R.W. and X.O.B.), NCI P01 CA69246 (X.O.B.), and NINDS P30NS045776 (X.O.B.); and the Brain Tumor Society (A.M.K.). We thank E. Erkan, L. Wedekind, and P. Waterman for technical assistance and G.S. Mack for critical reading of the manuscript.

Jürgen Soutschek is an employee and shareholder of Regulus Therapeutics.

Received: December 18, 2007
Revised: August 23, 2008
Accepted: October 9, 2008
Published: November 3, 2008

REFERENCES

Ambros, V. (2004). The functions of animal microRNAs. Nature *431*, 350–355.

Bache, K.G., Raiborg, C., Mehlum, A., and Stenmark, H. (2003). STAM and Hrs are subunits of a multivalent ubiquitin-binding complex on early endosomes. J. Biol. Chem. *278*, 12513–12521.

Bartel, D.P. (2004). MicroRNAs: genomics, biogenesis, mechanism, and function. Cell *116*, 281–297.

Batchelor, T.T., Sorensen, A.G., di Tomaso, E., Zhang, W.T., Duda, D.G., Cohen, K.S., Kozak, K.R., Cahill, D.P., Chen, P.J., Zhu, M., et al. (2007). AZD2171, a pan-VEGF receptor tyrosine kinase inhibitor, normalizes tumor vasculature and alleviates edema in glioblastoma patients. Cancer Cell *11*, 83–95.

Brem, S., Cotran, R., and Folkman, J. (1972). Tumor angiogenesis: a quantitative method for histologic grading. J. Natl. Cancer Inst. *48*, 347–356.

Calin, G.A., and Croce, C.M. (2006). MicroRNA signatures in human cancers. Nat. Rev. Cancer *6*, 857–866.

Chen, C., Chai, H., Wang, X., Jiang, J., Jamaluddin, M.S., Liao, D., Zhang, Y., Wang, H., Bharadwaj, U., Zhang, S., et al. (2008). Soluble CD40 ligand induces endothelial dysfunction in human and porcine coronary artery endothelial cells. Blood *112*, 3205–3216.

de Fougerolles, A., Vornlocher, H.P., Maraganore, J., and Lieberman, J. (2007). Interfering with disease: a progress report on siRNA-based therapeutics. Nat. Rev. Drug Discov. *6*, 443–453.

Dews, M., Homayouni, A., Yu, D., Murphy, D., Sevignani, C., Wentzel, E., Furth, E.E., Lee, W.M., Enders, G.H., Mendell, J.T., et al. (2006). Augmentation of tumor angiogenesis by a Myc-activated microRNA cluster. Nat. Genet. *38*, 1060–1065.

Esquela-Kerscher, A., and Slack, F.J. (2006). Oncomirs - microRNAs with a role in cancer. Nat. Rev. Cancer *6*, 259–269.

Ewan, L.C., Jopling, H.M., Jia, H., Mittar, S., Bagherzadeh, A., Howell, G.J., Walker, J.H., Zachary, I.C., and Ponnambalam, S. (2006). Intrinsic tyrosine kinase activity is required for vascular endothelial growth factor receptor 2 ubiquitination, sorting and degradation in endothelial cells. Traffic *7*, 1270–1282.

Fish, J.E., Santoro, M.M., Morton, S.U., Yu, S., Yeh, R.F., Wythe, J.D., Ivey, K.N., Bruneau, B.G., Stainier, D.Y., and Srivastava, D. (2008). miR-126 regulates angiogenic signaling and vascular integrity. Dev. Cell *15*, 272–284.

Folkerth, R.D. (2000). Descriptive analysis and quantification of angiogenesis in human brain tumors. J. Neurooncol. *50*, 165–172.

Folkman, J. (2007). Angiogenesis: an organizing principle for drug discovery? Nat. Rev. Drug Discov. *6*, 273–286.

Griffiths-Jones, S., Grocock, R.J., van Dongen, S., Bateman, A., and Enright, A.J. (2006). miRBase: microRNA sequences, targets and gene nomenclature. Nucleic Acids Res. *34*, D140–D144.

Grimm, J., Kirsch, D.G., Windsor, S.D., Kim, C.F., Santiago, P.M., Ntziachristos, V., Jacks, T., and Weissleder, R. (2005). Use of gene expression profiling to direct in vivo molecular imaging of lung cancer. Proc. Natl. Acad. Sci. USA *102*, 14404–14409.

Haglund, K., Sigismund, S., Polo, S., Szymkiewicz, I., Di Fiore, P.P., and Dikic, I. (2003). Multiple monoubiquitination of RTKs is sufficient for their endocytosis and degradation. Nat. Cell Biol. *5*, 461–466.

Jackson, A.L., Bartz, S.R., Schelter, J., Kobayashi, S.V., Burchard, J., Mao, M., Li, B., Cavet, G., and Linsley, P.S. (2003). Expression profiling reveals off-target gene regulation by RNAi. Nat. Biotechnol. *21*, 635–637.

Jain, R.K. (2005). Normalization of tumor vasculature: an emerging concept in antiangiogenic therapy. Science *307*, 58–62.

John, B., Enright, A.J., Aravin, A., Tuschl, T., Sander, C., and Marks, D.S. (2004). Human MicroRNA targets. PLoS Biol. *2*, e363.

Kerbel, R., and Folkman, J. (2002). Clinical translation of angiogenesis inhibitors. Nat. Rev. Cancer *2*, 727–739.

Khodarev, N.N., Yu, J., Labay, E., Darga, T., Brown, C.K., Mauceri, H.J., Yassari, R., Gupta, N., and Weichselbaum, R.R. (2003). Tumour-endothelium interactions in co-culture: coordinated changes of gene expression profiles and phenotypic properties of endothelial cells. J. Cell Sci. *116*, 1013–1022.

Kloosterman, W.P., and Plasterk, R.H. (2006). The diverse functions of microRNAs in animal development and disease. Dev. Cell *11*, 441–450.

Krek, A., Grun, D., Poy, M.N., Wolf, R., Rosenberg, L., Epstein, E.J., MacMenamin, P., da Piedade, I., Gunsalus, K.C., Stoffel, M., and Rajewsky, N. (2005). Combinatorial microRNA target predictions. Nat. Genet. *37*, 495–500.

Krichevsky, A.M., King, K.S., Donahue, C.P., Khrapko, K., and Kosik, K.S. (2003). A microRNA array reveals extensive regulation of microRNAs during brain development. RNA *9*, 1274–1281.

Krutzfeldt, J., Rajewsky, N., Braich, R., Rajeev, K.G., Tuschl, T., Manoharan, M., and Stoffel, M. (2005). Silencing of microRNAs in vivo with 'antagomirs'. Nature *438*, 685–689.

Kuehbacher, A., Urbich, C., Zeiher, A.M., and Dimmeler, S. (2007). Role of Dicer and Drosha for endothelial microRNA expression and angiogenesis. Circ. Res. *101*, 59–68.

Lee, D.Y., Deng, Z., Wang, C.H., and Yang, B.B. (2007). MicroRNA-378 promotes cell survival, tumor growth, and angiogenesis by targeting SuFu and Fus-1 expression. Proc. Natl. Acad. Sci. USA *104*, 20350–20355.

Lewis, B.P., Burge, C.B., and Bartel, D.P. (2005). Conserved seed pairing, often flanked by adenosines, indicates that thousands of human genes are microRNA targets. Cell *120*, 15–20.

Miebach, S., Grau, S., Hummel, V., Rieckmann, P., Tonn, J.C., and Goldbrunner, R.H. (2006). Isolation and culture of microvascular endothelial cells from gliomas of different WHO grades. J. Neurooncol. *76*, 39–48.

Miranda, K.C., Huynh, T., Tay, Y., Ang, Y.S., Tam, W.L., Thomson, A.M., Lim, B., and Rigoutsos, I. (2006). A pattern-based method for the identification of MicroRNA binding sites and their corresponding heteroduplexes. Cell *126*, 1203–1217.

Montet, X., Ntziachristos, V., Grimm, J., and Weissleder, R. (2005). Tomographic fluorescence mapping of tumor targets. Cancer Res. *65*, 6330–6336.

Montet, X., Figueiredo, J.L., Alencar, H., Ntziachristos, V., Mahmood, U., and Weissleder, R. (2007). Tomographic fluorescence imaging of tumor vascular volume in mice. Radiology *242*, 751–758.

Ntziachristos, V., Tung, C.H., Bremer, C., and Weissleder, R. (2002). Fluorescence molecular tomography resolves protease activity in vivo. Nat. Med. *8*, 757–760.

Poliseno, L., Tuccoli, A., Mariani, L., Evangelista, M., Citti, L., Woods, K., Mercatanti, A., Hammond, S., and Rainaldi, G. (2006). MicroRNAs modulate the angiogenic properties of HUVECs. Blood *108*, 3068–3071.

Raiborg, C., Bache, K.G., Gillooly, D.J., Madshus, I.H., Stang, E., and Stenmark, H. (2002). Hrs sorts ubiquitinated proteins into clathrin-coated microdomains of early endosomes. Nat. Cell Biol. *4*, 394–398.

Reich, S.J., Fosnot, J., Kuroki, A., Tang, W., Yang, X., Maguire, A.M., Bennett, J., and Tolentino, M.J. (2003). Small interfering RNA (siRNA) targeting VEGF effectively inhibits ocular neovascularization in a mouse model. Mol. Vis. *9*, 210–216.

Rizzo, M.A., Springer, G.H., Granada, B., and Piston, D.W. (2004). An improved cyan fluorescent protein variant useful for FRET. Nat. Biotechnol. *22*, 445–449.

Ruvkun, G. (2006). Clarifications on miRNA and cancer. Science *311*, 36–37.

Shen, J., Samul, R., Silva, R.L., Akiyama, H., Liu, H., Saishin, Y., Hackett, S.F., Zinnen, S., Kossen, K., Fosnaugh, K., et al. (2006). Suppression of ocular neovascularization with siRNA targeting VEGF receptor 1. Gene Ther. *13*, 225–234.

Shih, A.H., and Holland, E.C. (2006). Platelet-derived growth factor (PDGF) and glial tumorigenesis. Cancer Lett. *232*, 139–147.

Stern, K.A., Visser Smit, G.D., Place, T.L., Winistorfer, S., Piper, R.C., and Lill, N.L. (2007). Epidermal growth factor receptor fate is controlled by Hrs tyrosine

phosphorylation sites that regulate Hrs degradation. Mol. Cell. Biol. *27*, 888–898.

Suárez, Y., Fernandez-Hernando, C., Pober, J.S., and Sessa, W.C. (2007). Dicer dependent microRNAs regulate gene expression and functions in human endothelial cells. Circ. Res. *100*, 1164–1173.

Takata, H., Kato, M., Denda, K., and Kitamura, N. (2000). A hrs binding protein having a Src homology 3 domain is involved in intracellular degradation of growth factors and their receptors. Genes Cells *5*, 57–69.

Tuccoli, A., Poliseno, L., and Rainaldi, G. (2006). miRNAs regulate miRNAs: coordinated transcriptional and post-transcriptional regulation. Cell Cycle *5*, 2473–2476.

Wang, S., Aurora, A.B., Johnson, B.A., Qi, X., McAnally, J., Hill, J.A., Richardson, J.A., Bassel-Duby, R., and Olson, E.N. (2008). The endothelial-specific microRNA miR-126 governs vascular integrity and angiogenesis. Dev. Cell *15*, 261–271.

Wurdinger, T., and Costa, F.F. (2007). Molecular therapy in the microRNA era. Pharmacogenomics J. *7*, 297–304. Published online December 26, 2006. 10.1038/sj.tpj.6500429.